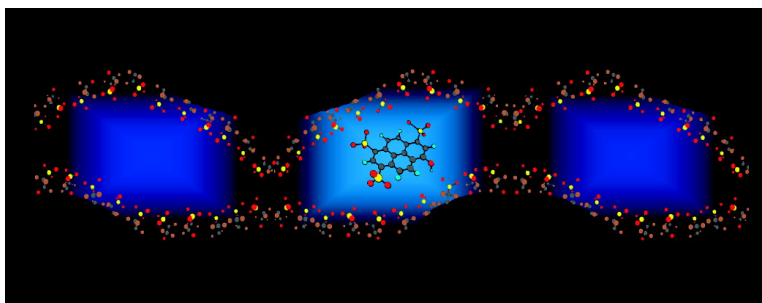


## Proton Transport and the Water Environment in Nafion Fuel Cell Membranes and AOT Reverse Micelles

D. B. Spry, A. Goun, K. Glusac, David E. Moilanen, and M. D. Fayer

*J. Am. Chem. Soc.*, **2007**, 129 (26), 8122-8130 • DOI: 10.1021/ja071939o • Publication Date (Web): 13 June 2007

Downloaded from <http://pubs.acs.org> on February 16, 2009



### More About This Article

Additional resources and features associated with this article are available within the HTML version:

- Supporting Information
- Links to the 8 articles that cite this article, as of the time of this article download
- Access to high resolution figures
- Links to articles and content related to this article
- Copyright permission to reproduce figures and/or text from this article

[View the Full Text HTML](#)

## Proton Transport and the Water Environment in Nafion Fuel Cell Membranes and AOT Reverse Micelles

D. B. Spry, A. Goun, K. Glusac, David E. Moilanen, and M. D. Fayer\*

Contribution from the Department of Chemistry, Stanford University, Stanford, California 94305

Received March 19, 2007; E-mail: fayer@stanford.edu

**Abstract:** The properties of confined water and diffusive proton-transfer kinetics in the nanoscopic water channels of Nafion fuel cell membranes at various hydration levels are compared to water in a series of well-characterized AOT reverse micelles with known water nanopool sizes using the photoacid pyranine as a molecular probe. The side chains of Nafion are terminated by sulfonate groups with sodium counterions that are arrayed along the water channels. AOT has sulfonate head groups with sodium counterions that form the interface with the reverse micelle's water nanopool. The extent of excited-state deprotonation is observed by steady-state fluorescence measurements. Proton-transfer kinetics and orientational relaxation are measured by time-dependent fluorescence using time-correlated single photon counting. The time dependence of deprotonation is related to diffusive proton transport away from the photoacid. The fluorescence reflecting the long time scale proton transport has an  $\sim t^{-0.8}$  power law decay in contrast to bulk water, which has a  $t^{-3/2}$  power law. For a given hydration level of Nafion, the excited-state proton transfer and the orientational relaxation are similar to those observed for a related size AOT water nanopool. The effective size of the Nafion water channels at various hydration levels are estimated by the known size of the AOT reverse micelles that display the corresponding proton-transfer kinetics and orientational relaxation.

### Introduction

Nafion is a perfluorosulfonate polymer developed by DuPont that was originally designed as a permselective membrane separator in chlor-alkali cells.<sup>1</sup> Currently, the largest interest in Nafion is driven by its use as a proton conducting membrane in fuel cells. Nafion membranes in fuel cells allow protons to diffuse from the anode to the cathode to complete an electrochemical circuit, but they prevent the reactant gases from passing through the membrane.

The repeat structure of Nafion is given in Figure 1A. For these experiments, Na<sup>+</sup> is used for the counterion. The polymer consists of a nonpolar fluorinated backbone and a polar side chain. The difference in polarity of these two groups results in the formation of segregated hydrophobic and hydrophilic nanoscopic domains. The hydrophilic regions form an interconnected network that upon hydration allows protons to flow.<sup>2–5</sup> The selectivity of ion diffusion of Nafion,<sup>6</sup> as well as other permselective membranes,<sup>7</sup> has been shown to be highly sensitive to both the geometric and chemical composition of

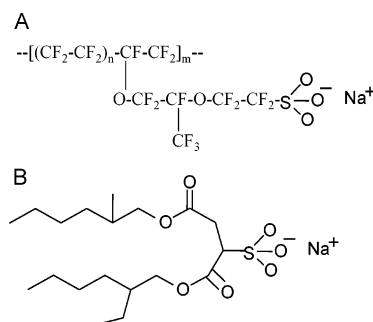


**Figure 1.** (A) Repeat structure of Nafion.  $n$  can vary between 5 and 14, and  $m$  is typically on the order of 1000. (B) Structure of Aerosol OT (AOT).

the hydrophilic network.<sup>8</sup> It is apparent that designing these materials for optimum performance requires a detailed knowledge of the nanoscopic chemical environment as well as a molecular level view of proton transport inside the channels. In addition, explicating the nature of water and proton transport in Nafion nanochannels is a guide to understanding the influence of nanoconfinement on proton transport and other processes.

One of the first attempts to describe the structure of Nafion was the cluster-network model.<sup>4</sup> This model was largely based on small-angle neutron scattering studies and concluded that the morphology of Nafion consists of ionic sulfonate clusters that are approximately spherical in shape and resemble reverse micelles. These reverse micelle structures were thought to be connected by narrow channels lined with sulfonate groups that

- (1) Hora, C. J.; Maloney, D. E. *J. Electrochem. Soc.* **1977**, *124*, C319.
- (2) Rubatat, L.; Rollet, A. L.; Gebel, G.; Diat, O. *Macromolecules* **2002**, *35*, 4050–4055.
- (3) Gebel, G.; Lambard, J. *Macromolecules* **1997**, *30*, 7914–7920.
- (4) Gierke, T. D.; Munn, G. E.; Wilson, F. C. *J. Polym. Sci.: Polym. Phys. Ed.* **1981**, *19*, 1687–1704.
- (5) Zawodzinski, T. A., Jr.; Derouin, C.; Radzinski, S.; Sherman, R. J.; Smith, T. V.; Springer, T. E.; Gottesfeld, S. *J. Electrochem. Soc.* **1993**, *140*, 1041–1047.
- (6) Zawodzinski, T. A., Jr.; Neeman, M.; Sillerud, L. O.; Gottesfeld, S. *J. Phys. Chem.* **1991**, *95*, 6040–6044.
- (7) Eisenberg, A.; Yeager, H. L. In *ACS Symposium Series*; Eisenberg, A., Yeager, H. L., Eds.; American Chemical Society: Washington, DC, 1982; No. 180, p 500.

- (8) Mauritz, K. A.; Moore, R. B. *Chem. Rev.* **2004**, *104*, 4535–4585.

permit the migration of positive ions but stop the flow of negatively charged ions. Through a wealth of information obtained in the past several decades, primarily from scattering<sup>4,9,10</sup> and microscopy<sup>11–13</sup> studies, there have been many modifications of this simple description. However, most models still consist of larger hydrophilic domains, whose approximate size can range from 1 to 5 nm with increasing water content, and smaller hydrophilic channels that enabled the transport of ions between different water pools. In recent years, the view of the hydrophilic network of Nafion has shifted from a well-defined reverse micelle structure to domains of irregular channels with random connectivity that swell upon hydration.<sup>2,8,14,15</sup>

In this paper we investigate the aqueous environment in Nafion membrane channels at various hydration levels by comparing a variety of measurements to a reverse micelle system of similar chemical composition. In doing so it is possible to contrast the nanoscopic water environments of the two systems and evaluate the usefulness of the simple reverse micelle model to describe the aqueous chemical environment of Nafion channels.<sup>4,16</sup> In addition, information is obtained on the nature of proton transport inside Nafion channels in relation to the same observations in bulk water.

Water in Nafion channels is compared to the nanoscopic water pools in reverse micelles made with the anionic surfactant Aerosol OT (AOT, shown in Figure 1B) in the organic phase heptane. AOT/heptane reverse micelles are known to be spherical at room temperature. The size of the reverse micelle is adjustable by varying the mole ratio,  $w_o$ , of water molecules to surfactant molecules

$$w_o = \frac{n_{\text{H}_2\text{O}}}{n_{\text{AOT}}} \quad (1)$$

where  $n$  is the number of moles. The water nanopools of AOT reverse micelles provide a useful environment to compare to the water domains of hydrated Nafion membranes because both systems contain the same ionic sulfonate functional group that separates the hydrophilic and hydrophobic regions. Furthermore, AOT reverse micelles have been characterized by a variety of techniques and have been shown to form well-defined spherical structures with low (size) polydispersity at a given  $w_o$  value.<sup>17,18</sup> The linear size relationship

$$d_{\text{wp}} = 0.29w_o + 1.1 \text{ (nm)} \quad (2)$$

gives the diameter of the nanopool and applies below  $w_o = 20$ .<sup>19</sup> The size of water pools in larger reverse micelles is also known.<sup>20</sup>

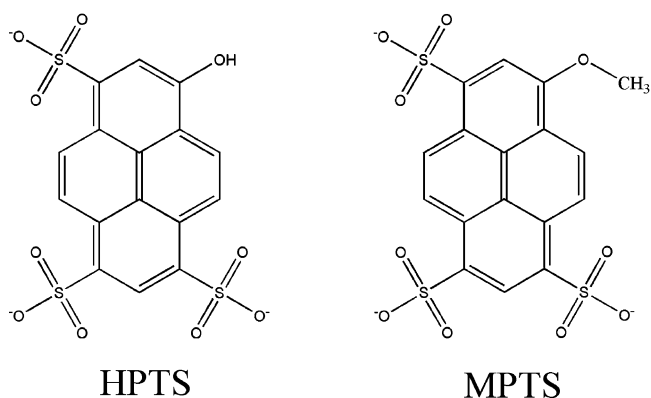


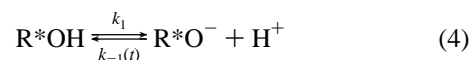
**Figure 2.** Structures of pyranine (1-hydroxy-3,6,8-pyrenetrisulfonic acid, commonly referred to as HPTS) and MPTS, the methoxy derivative of HPTS.

The  $w_o$  value gives a convenient scale to compare AOT reverse micelles to Nafion at different hydration levels. The number of water molecules per sulfonate group in Nafion,  $\lambda$

$$\lambda = \frac{n_{\text{H}_2\text{O}}}{n_{\text{SO}_3^-}} \quad (3)$$

is a parameter used to characterize the state of hydration. The value of  $\lambda$  can be controlled, which influences the size of the hydrophilic domains and affects many of the important physical characteristics of Nafion, such as proton conductivity and molecular diffusion through the water channels.<sup>6</sup>

The molecular probes 8-hydroxypyrene-1,3,6-trisulfonate (HPTS or pyranine) and its methoxy derivative, 8-hydroxypyrene-1,3,6-trisulfonate (MPTS) are used to probe the water environment of Nafion and compare to that of AOT reverse micelles. HPTS undergoes a dramatic change in its acidity upon electronic excitation. The ground-state  $\text{pK}_a$  of HPTS is 7.7, which results in it being primarily protonated in neutral bulk water. Upon photoexcitation the  $\text{pK}_a$  drops approximately 7 units and HPTS rapidly transfers a proton to the surrounding solvent.<sup>21–23</sup>



The dynamics of proton transfer is dramatically affected by the ability of the solvent to reorganize and solvate the ion pair formed in the reaction. Since the reaction is reversible, the observed dynamics also depends on the proton mobility, that is, the ability of the hydronium ion to move away from the resulting anion. These properties make excited-state proton transfer (ESPT) a convenient probe for the local water environment and proton transport in nanoporous materials. For Nafion, proton transfer is particularly important because it is Nafion's primary function in fuel cells.

A serious complication for using molecular probes to study heterogeneous environments is in knowing how the molecules partition into different local regions of the sample. HPTS is a

- (9) Roche, E. J.; Pineri, M.; Duplessix, R. *J. Polym. Sci.: Polym. Phys.* **1982**, *20*, 107–116.  
 (10) Litt, M. H. *Polym. Prepr. (Am. Chem. Soc., Div. Polym. Chem.)* **1997**, *38*, 80.  
 (11) Rieberer, S.; Norian, K. H. *Ultramicroscopy* **1992**, *41*, 225–233.  
 (12) Ceynowa, J. *Polymer* **1978**, *19*, 73–76.  
 (13) Xue, T.; Trent, J. S.; Osseo-Asare, K. *J. Membr. Sci.* **1989**, *45*, 261–271.  
 (14) Falk, M. *Can. J. Chem.* **1980**, *58*, 1495–1501.  
 (15) Blake, N. P.; Petersen, M. K.; Voth, G. A.; Metiu, H. *J. Phys. Chem. B* **2005**, *109*, 24244–24253.  
 (16) Hsu, W. Y.; Gierke, T. D. *Macromolecules* **1982**, *15*, 101–105.  
 (17) Magid, L. J.; Daus, K. A.; Butler, P. D.; Quincy, R. B. *J. Phys. Chem.* **1983**, *87*, 5472–5478.  
 (18) Eicke, H.-F.; Kubik, R.; Hammerich, H. J. *J. Colloid Interface Sci.* **1982**, *90*, 27–33.  
 (19) Zulauf, M.; Eicke, H.-F. *J. Phys. Chem.* **1979**, *83*, 480–486.

- (20) Kinugasa, T.; Kondo, A.; Nishimura, S.; Miyauchi, Y.; Nishii, Y.; Watanabe, K.; Takeuchi, H. *Colloids Surf., A: Physicochem. Eng. Aspects* **2002**, *204*, 193–199.  
 (21) Spry, D. B.; Goun, A.; Fayer, M. D. *J. Chem. Phys.* **2006**, *125*, 144514.  
 (22) Leiderman, P.; Genosar, L.; Huppert, D. *J. Phys. Chem. A* **2005**, *109*, 5965–5977.  
 (23) Pines, E.; Huppert, D. *J. Chem. Phys.* **1986**, *84*, 3576–3577.

particularly useful probe for water because of its large  $-3$  formal charge, which forces it to reside almost exclusively in the aqueous phase where it can be well solvated. In the reverse micelles, the negative charge of the sulfonate head groups at the interface with the water nanopool provides a Coulombic repulsion that keeps the HPTS from diffusing into the interfacial region. For this reason, HPTS has been used in several previous studies to investigate the water environment in AOT reverse micelles<sup>24–26</sup> as well the encapsulated water in other anionic surfactants.<sup>27,28</sup>

Time-resolved IR studies of the OD stretch of HOD in H<sub>2</sub>O have shown that the dynamics of water slow considerably upon nanoconfinement in AOT reverse micelles<sup>29,30</sup> and Nafion membranes.<sup>29,31</sup> The linear IR spectrum for the OD stretch of water blue-shifts significantly in hydrated Nafion membranes and AOT reverse micelles smaller than  $w_o = 20$ , which corresponds to a water pool less than 7 nm in diameter. Similar observations of water in Nafion have been made by Faulk.<sup>14</sup> Of particular interest here are ultrafast IR orientational relaxation experiments on nanoscopic water in AOT<sup>32–35</sup> and in Nafion.<sup>29,31</sup> In AOT it was determined that, for small nanopools, water orientational relaxation is much slower than in bulk water and becomes increasingly slow as the size is decreased. In addition, in contrast to bulk water, orientational relaxation is not single exponential. Similar results were found in Nafion as a function of the level of hydration of the membrane. Orientational relaxation at very low levels of hydration was extremely slow, and even at the highest level of hydration studied,  $\lambda = 7.5$ , orientational relaxation is biexponential with the time constant for complete orientational randomization of 17 ps in contrast to 2.6 ps in bulk water. For water to undergo orientational relaxation, hydrogen bonds must break and re-form in a new geometry resulting in the OD bond vector of HOD pointing in a different direction. The slow rates of water orientational relaxation in nanoscopic water environments demonstrate that the time scale for hydrogen bond network rearrangement is slowed down substantially. Because processes in water, such as proton transport or orientational relaxation of a probe molecule, depend on hydrogen bond rearrangement, the results of the experiments on nanoscopic water indicate that processes occurring in nanowater will be significantly different from the same processes in bulk water.

There have been several previous attempts to study the aqueous environment of Nafion using molecular probes.<sup>36–40</sup>

Most studies have looked at fully hydrated or completely dry Nafion. Furthermore, because of the choice of a nonpolar or slightly polar molecule, many of these studies are complicated by the uncertainty of where the molecule resides. In this study, we gain a better understanding of the water environment of Nafion with varying the hydration levels by using a probe that preferentially resides in the deepest part of the water pools. In addition, direct comparisons with the identical experiments on the well-characterized AOT nanopools provide important information and insights into the nature of Nafion water channels and proton transfer in the channels.

## Experimental Procedures

Nafion 117 membranes were purchased from Fuelstore.com in the acid form. The samples were soaked for 24 h in a 1 M NaCl solution followed by a deionized water rinse to exchange the acidic protons for sodium ions. The Nafion samples were then boiled for 24 h in a  $\sim 0.1$  M solution of HPTS or MPTS (see Figure 2) to incorporate the molecular probe into the membrane. A home-built humidity system was used to control the hydration level of the Nafion samples. First the samples were dried. Then, air, with relative humidity that could be adjusted from 0 to 100%, was circulated through a sealed Plexiglas box with glove ports for sample manipulation. An internal humidity meter was used measure the relative humidity level, which was kept constant. The number of water molecules per sulfonate,  $\lambda$ , was determined by measuring the mass uptake of Nafion as a function of relative humidity. After samples reached the proper hydration level, they were sealed in a 1 mm fused silica cuvette while still in the humidity control box to retain a constant humidity level.

Aerosol OT, hexane (Aldrich Inc.), and deionized water were used without further purification. A 0.5 M stock solution of AOT in *n*-heptane was prepared. To prepare solutions of desired  $w_o$  value, precise amounts of water with either HPTS or MPTS already incorporated were added to measured quantities of the stock solution. The concentrations of HPTS and MPTS were kept below  $10^{-5}$  M to ensure that no more than one dye molecule occupied the same reverse micelle.

Fluorescence spectra were taken on a Fluorolog-3 fluorescence spectrometer. The fluorescence measurements were made at low concentration to avoid spectral distortion from emission reabsorption. The spectra were corrected for the Xe lamp intensity profile, monochromator, and photomultiplier response.

A Ti:sapphire oscillator was used as the excitation source in the time-correlated single photon counting (TCSPC) experiments. The laser wavelength was set to 790 nm and the output beam was focused into an acoustooptic pulse selector, which produced pulses at 4 MHz. The single pulses were frequency doubled and used for excitation. Excitation polarization was controlled by a half-wave plate placed immediately before the sample. The emitted photons were collected with a front-face geometry and passed through a fixed-angle polarizer before entering a monochromator. The photons were detected with a Hamamatsu microchannel plate detector. The instrument response function was  $\sim 45$  ps full width at half-maximum. All measurements were carried out at room temperature. The time to amplitude converter and multichannel analyzer were calibrated using an EG&G Ortec 462 time calibrator.

The TCSPC measurements for excited-state proton-transfer dynamics were made by rotating the polarization of the excitation beam to the magic angle ( $54.7^\circ$ ) with respect to the collecting polarizer. The

- (24) Bardez, E.; Goguillon, B.-T.; Keh, E.; Valeur, B. *J. Phys. Chem.* **1984**, *88*, 1909–1913.  
 (25) Kondo, H.; Miwa, I.; Sunamoto, J. *J. Phys. Chem.* **1982**, *86*, 4826–4831.  
 (26) Politi, M. J.; Chaimovich, H. *J. Phys. Chem.* **1986**, *90*, 282–287.  
 (27) Clement, N. R.; Gould, J. M. *Biochemistry* **1981**, *20*, 1534–1538.  
 (28) Kano, K.; Fendler, J. H. *Chem. Phys. Lipids* **1979**, *23*, 189–200.  
 (29) Moilanen, D. E.; Piletic, I. R.; Fayer, M. D. *J. Phys. Chem. A* **2006**, *110*, 9084–9088.  
 (30) Piletic, I. R.; Tan, H.-S.; Fayer, M. D. *J. Phys. Chem. B* **2005**, *109*, 21273–21284.  
 (31) Moilanen, D. E.; Piletic, I. R.; Fayer, M. D. *J. Phys. Chem. C*, published online March 7, 2007, <http://dx.doi.org/10.1021/jp067460k>.  
 (32) Piletic, I. R.; Moilanen, D. E.; Spry, D. B.; Levinger, N. E.; Fayer, M. D. *J. Phys. Chem. A* **2006**, *110*, 4985–4999.  
 (33) Piletic, I. R.; Moilanen, D. E.; Levinger, N. E.; Fayer, M. D. *J. Am. Chem. Soc.* **2006**, *128*, 10366–10367.  
 (34) Tan, H.-S.; Piletic, I. R.; Riter, R. E.; Levinger, N. E.; Fayer, M. D. *Phys. Rev. Lett.* **2004**, *94*, 057405 (057404).  
 (35) Tan, H.-S.; Piletic, I. R.; Fayer, M. D. *J. Chem. Phys.* **2005**, *122*, 174501 (174509).  
 (36) Mukherjee, T. K.; Datta, A. *J. Phys. Chem. B* **2005**, *110*, 2611–2617.  
 (37) Szentirmay, M. N.; Prieto, N. E.; Martin, C. R. *J. Phys. Chem.* **1985**, *89*, 3017–3023.

- (38) Lee, H. W. H.; Huston, A. L.; Gehrtz, M.; Moerner, W. E. *Chem. Phys. Lett.* **1985**, *114*, 491–496.  
 (39) Kalyanasundaram, K.; Thomas, J. K. *J. Am. Chem. Soc.* **1977**, *99*, 2039–2044.  
 (40) Kuczynski, J. P.; Milovsavljevic, B. H.; Thomas, J. K. *J. Phys. Chem.* **1984**, *84*, 980–984.

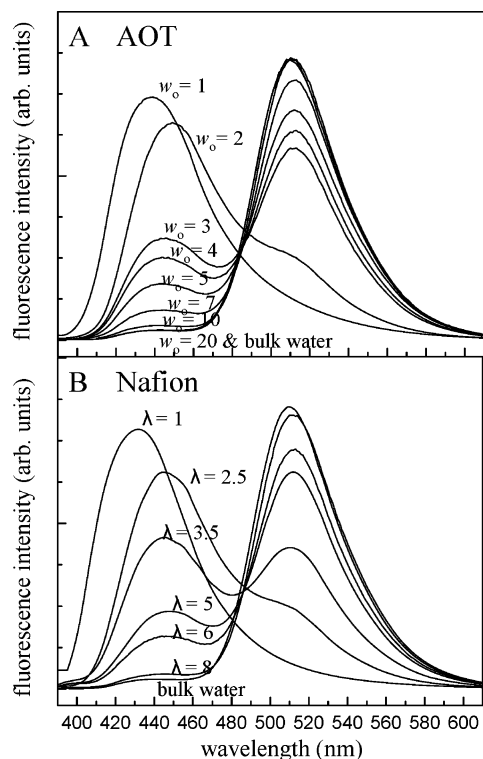


**Figure 3.** Steady-state fluorescence spectra of (A) HPTS in AOT and (B) HPTS in Nafion.

anisotropy measurements of MPTS were carried out by setting the excitation polarization to  $0^\circ$  and  $90^\circ$  to measure the parallel and perpendicularly polarized fluorescence decays, denoted as  $I_{\parallel}(t)$  and  $I_{\perp}(t)$ , respectively. The time-dependent polarized fluorescence intensities can be expressed as

$$I_{\parallel}(t) = P(t)(1 + 0.8C(t)) \quad (5)$$

$$I_{\perp}(t) = P(t)(1 - 0.4C(t)) \quad (6)$$

where  $P(t)$  is the excited-state population decay and  $C(t)$  is the second Legendre polynomial dipole orientational correlation function. The orientational relaxation can be separated from the population dynamics by defining the time-dependent anisotropy as

$$r(t) = \frac{I_{\parallel}(t) - I_{\perp}(t)}{I_{\parallel}(t) + 2I_{\perp}(t)} \quad (7)$$

which yields

$$r(t) = 0.4C(t) \quad (8)$$

## Results and Discussion

**Proton-Transfer Dynamics.** Figure 3A shows the fluorescence spectra of HPTS in a series of AOT reverse micelles and bulk water. The protonated state's fluorescence maximum appears at 445 nm in situations where enough water is present to solvate the molecule (all samples except  $w_o = 1$ ) and the deprotonated state's maximum is at 510 nm.

These results are in agreement with previous reports.<sup>24</sup> For the nanoscopic water pools in reverse micelles greater than  $w_o = 10$ , the extent of excited-state deprotonation is virtually the same as in pure water. This fact provides evidence that the HPTS molecule resides in the aqueous phase and not in the reverse micelle wall or other nonpolar environment. A  $w_o = 10$  AOT

reverse micelle has a water pool radius of  $\sim 2$  nm, which is not large when compared to the hygroscopic radius of HPTS (0.5 nm).<sup>41</sup> This leaves a maximum distance from the HPTS molecule to the micelle wall of 1.5 nm. Even for HPTS located on average in the center of the water pool, when one considers the statistical fluctuations about the average, the most probable distance from HPTS to the wall is most likely smaller.

The changes in the spectra of HPTS in AOT reverse micelles with decreasing size has led some authors<sup>25,26</sup> to conclude that two types of water environments exist. One type of water has bulk characteristics (core of the water pool), and the other type is in the interfacial region is much less mobile (interfacial shell). When the AOT micelles shrink below a certain size, the HPTS molecule is forced to reside in the interfacial water. In this environment, the water molecules cannot solvate the charge pair formed in the reaction as effectively and reduce the extent of excited-state proton transfer. However, recent ultrafast infrared experiments performed on the water nanopools of AOT can provide an alternative explanation for the size dependence.<sup>32</sup> The shell of water has a different structure from that of bulk water. The hydrogen bond network couples the water in the shell to the water in the core of the reverse micelle. The coupled network has dynamics which are distinct from those of bulk water in small reverse micelles. For large reverse micelle nanopools, the core is so large that it has bulk-like properties, but as the nanopool becomes small, the coupled core-shell hydrogen bond network has hydrogen bond dynamics that are substantially slower than those of bulk water.<sup>30,32,34,35</sup> Again, the modified hydrogen bond network of small reverse micelles results in water molecules that cannot solvate the charge pair as effectively and reduce the extent of excited-state proton transfer.

Figure 3B shows the same trend for Nafion. As the membrane becomes more hydrated (larger  $\lambda$ ), HPTS can more readily undergo ESPT. Again, at very low hydration ( $\lambda = 1$ ) there is reduced solvation of HPTS and the fluorescence spectrum is blue-shifted relative to the spectra at higher hydration levels. There is a qualitative correlation between the fluorescence spectra of AOT and Nafion with respect to the hydration level. In both systems, the number of water molecules per sulfonate group strongly influences the extent of proton transfer. The similarity in the spectroscopic trends with the number of water molecules per sulfonate does not necessarily mean that the spherical nanopools of AOT reverse micelles are the same size as those found in Nafion membranes at the same equivalent hydration level. What the results suggest is that, in Nafion, HPTS is in a water environment that is analogous to that found in AOT at similar hydration levels.

More information can be obtained about the proton transport process in Nafion and the nature of the Nafion water channels by observing the time-resolved proton transport dynamics. The dissociation dynamics of HPTS have been studied extensively by a number of authors.<sup>22,42–45</sup> Proton dissociation leaves HPTS in an electronic excited state. Because of HPTS's negative

(41) Haar, H. P.; Klein, U. K. A.; Hafner, F. W.; Hauser, M. *Chem. Phys. Lett.* **1977**, *49*, 563–567.

(42) Mohammed, O. F.; Pines, D.; Dreyer, J.; Pines, E.; Nibbering, E. T. J. *Science* **2005**, *310*, 83–86.

(43) Agmon, N. *J. Phys. Chem. A* **2005**, *109*, 13–35.

(44) Pines, E.; Huppert, D. *Chem. Phys. Lett.* **1986**, *126*, 88–91.

(45) Spry, D. B.; Goun, A.; Fayer, M. D. *J. Phys. Chem. A* **2007**, *111*, 230–237.

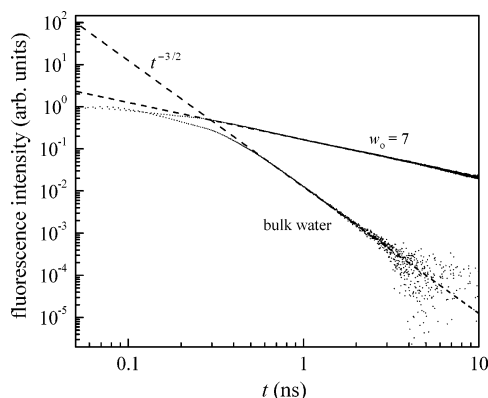


**Figure 4.** Protonated excited-state population of HPTS corrected for lifetime in bulk water and the water nanopools of  $w_0 = 7$  AOT reverse micelles. The dotted lines are included to show the  $t^{-3/2}$  power law decay in water and the  $\sim t^{-0.8}$  power law decay in the reverse micelle.

charge of 4 in the deprotonated state, the Coulombic attraction for the dissociated proton is large, and the recombination is substantial and fast in the excited state. (The ground-state recombination of the HPTS anion with a free hydronium ion is among the fastest measured bimolecular reactions.<sup>46</sup>)

The most common approach to modeling geminate recombination reactions is to employ the diffusion (Smoluchowski) equation with back-reaction boundary conditions.<sup>43,47,48</sup> This technique has been used to model the dynamics of photoacids in a number of different environments, including AOT reverse micelles.<sup>49</sup> This approach requires knowledge of the system's geometry, dielectric constant, proton diffusion constant, ion screening effects, and interactions at the boundary, all of which are unknown for Nafion. Nonetheless, it is possible to obtain substantial information about proton transport by comparing the proton transport dynamics of HPTS in AOT, Nafion, and bulk water through the use of an empirical model.

The long-time recombination rate,  $k_{-1}(t)$ , of two particles with a Coulomb potential has been obtained by solving the Smoluchowski equation analytically,<sup>50</sup> and has the form

$$k_{-1}(t) = k_{-1} t^{-d/2} \quad (9)$$

where  $d$  is the dimensionality of the diffusion. For the three-dimensional case

$$k_{-1} = \frac{R_D e^{-R_D/r_0}}{\sqrt{D}} \quad (10)$$

In eq 10,  $D$  is the combined diffusion constants of the two ions,  $R_D$  is the Debye radius, and  $r_0$  is the initial separation of the two ions immediately after dissociation has occurred.<sup>44,50</sup>

At long times relative to the initial dissociation time ( $\sim 1/k_{-1}$  in eq 4), the recombination kinetics determine the probability of finding the system in the protonated state of HPTS. In systems where free diffusion is possible in three dimensions, the time dependence goes as  $t^{-3/2}$ , the so-called "3/2 power law". The verification of this power law is shown in Figure 4, where it can be clearly seen on a logarithmic plot of the fluorescence

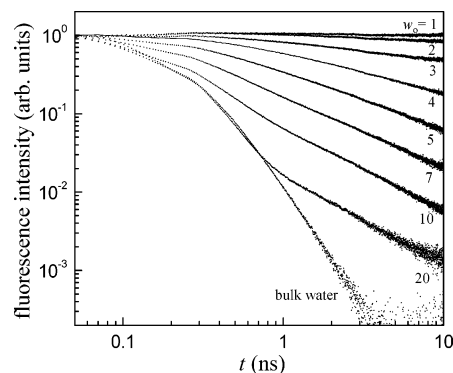


**Figure 5.** Lifetime-corrected fluorescence decay of HPTS in the water nanopools of the AOT samples studied. All reverse micelles with  $w_0 \geq 3$  display a power law decay with exponent  $\sim -0.8$ .

decay of the HPTS protonated state, corrected for the excited-state lifetime of HPTS in water by multiplying each curve by  $\exp(t/\tau)$ , where  $\tau = 5.4$  ns.<sup>22</sup> A dashed line with  $-3/2$  slope is included as an aid to the eye.

The dissociation dynamics of HPTS converge to the long-time limit in approximately  $\sim 0.5$  ns. The fluorescence decay of the protonated state of HPTS in  $w_0 = 7$  AOT reverse micelles is shown in the same plot for comparison. It is clear that the reverse micelle system also displays a power law, but the slope is much smaller ( $\sim 0.8$ ) than that found for pure water. In the spherical nanopool of the reverse micelle the diffusion is no longer occurring in an infinite three-dimensional system because of the finite size of the cavity. The Smoluchowski equation has been solved numerically in finite spheres,<sup>51</sup> but the analytical derivation of a power law has yet to be reported for such a system.

Figure 5 shows the lifetime-corrected fluorescence decay of the protonated state of HPTS in bulk water as well as in the entire series of AOT reverse micelles studied here. The extent of proton transfer is indistinguishable in the largest micelle size ( $w_0 = 20$ ) from bulk water by the steady-state fluorescence spectrum (see Figure 3A), but the time-resolved proton-transfer dynamics show a clear difference in the two systems.

At short times the ESPT dynamics for bulk water and  $w_0 = 20$  are nearly identical. At times of 1 ns or greater, the effect of confinement can be clearly seen. The radius of a  $w_0 = 20$  micelle is approximately 3.5 nm. The approximate time required for the ESPT dynamics of water and the  $w_0 = 20$  reverse micelle system to diverge is  $\sim 900$  ps. Using the proton diffusion constant of bulk water ( $\sim 10^{-4}$  cm<sup>2</sup>/s), it is found that the root-mean-square (rms) distance of proton displacement in 900 ps is 3 nm. Thus, the divergence occurs when the rms displacement is approximately the distance to the interface. While this is a qualitative argument, it demonstrates that the difference between bulk water and the  $w_0 = 20$  reverse micelles (and smaller) arises because of the finite extent of the nanopool. It also indicates that the proton transfer is initially very similar to that of bulk water, and that the HPTS molecule resides deep in the water phase away from the ionic reverse micelle interface. In general, all of the micelles larger than  $w_0 = 3$  show a power law dependence with an exponent near  $-0.8$ . In terms of eq 9, this exponent would correspond to a dimensionality for the diffusion of 1.6, although this is clearly a finite volume three-dimensional

(46) Förster, T.; Volker, S. *Chem. Phys. Lett.* **1975**, *34*, 1–6.

(47) Agmon, N.; Szabo, A. *J. Chem. Phys.* **1990**, *92*, 5270–5284.

(48) Goun, A.; Glusac, K.; Fayer, M. D. *J. Chem. Phys.* **2006**, *124*, 084504.

(49) Cohen, B.; Huppert, D.; Solntsev, K. M.; Tsfadia, Y.; Nachliel, E.; Gutman, M. *J. Am. Chem. Soc.* **2001**, *124*, 7539–7547.

(50) Hong, K. M.; Noolandi, J. *J. Chem. Phys.* **1978**, *68*, 5163–5171.

(51) Agmon, N. *J. Chem. Phys.* **1987**, *88*, 5639–5642.

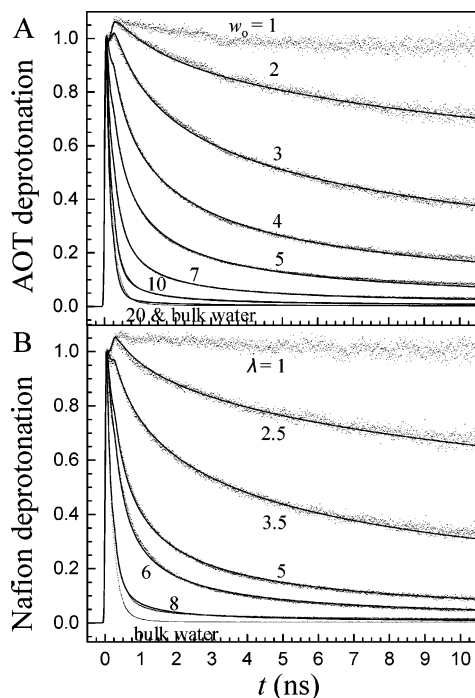


**Figure 6.** (A) Kinetic model fits to the fluorescence decays of HPTS in the water nanopools of AOT reverse micelles at various  $w_0$  values. (B) Kinetic model fits to HPTS in the water channels of Nafion at various  $\lambda$  values.

system rather than a system with a fractal dimension. The influences of finite volume on excitation transport systems that involve return to the initially excited molecule demonstrate the substantial effect finite volume has on transport observables.<sup>52–55</sup>

Because the majority of the reverse micelles display a power law with exponent of approximately  $-0.8$ , we empirically model the reverse reaction rate as  $k_{-1}(t) = k_{-1}t^{-0.8}$ . The population dynamics of the lifetime-corrected protonated state, RO\*H, in both the AOT and Nafion can then be fit to the rate equations.

$$\begin{pmatrix} \frac{d[\text{RO}^*\text{H}]}{dt} \\ \frac{d[\text{RO}^*]}{dt} \end{pmatrix} = \begin{pmatrix} -k_1 & k_{-1}t^{-0.8}[\text{RO}^*] \\ k_1 & -k_{-1}t^{-0.8}[\text{RO}^*] \end{pmatrix} \begin{pmatrix} [\text{RO}^*\text{H}] \\ [\text{RO}^*] \end{pmatrix} \quad (11)$$

This kinetic scheme produces an exponential decay at short times and a power law decay at long times. Equation 11 was integrated and fit to the TCSPC data in Figure 5 using least-squares regression. The resulting fits convolved with the instrument response are shown in parts A and B of Figure 6 for AOT and Nafion, respectively. Considering the simplicity of the model and given the wide range of samples having vastly different dynamics, the agreement between the data and the fits is very good.

The values of rate constants for the AOT reverse micelles and Nafion samples are given in Table 1. The time scale for the initial exponential decay of the protonated state in the largest AOT reverse micelle ( $1/k_1$ ) is  $\sim 100$  ps, which is in agreement with values that have been reported for bulk water.<sup>22,23,45</sup>

**Table 1.** ESPT Rate Constants of HPTS in AOT and Nafion

(A) HPTS in AOT		
$w_0$	$k_1$	$k_{-1}$
20	10	0.10
10	8.4	0.30
7	6.4	0.76
5	4.5	1.7
4	2.3	2.4
3	0.52	2.3
2	0.16	4.2
(B) HPTS in Nafion		
$\lambda$	$k_1$	$k_{-1}$
8	9.1	0.36
6	3.8	0.93
5	3.5	1.7
3.5	1.8	5.1
2.5	0.43	8.1

Both Nafion and AOT samples show the same trend: as the hydration level is reduced the rate of forward proton transfer decreases and the rate of the back reaction increases. The forward rate decreases as the size of the water pool becomes smaller because water cannot solvate the charge pair formed in the proton-transfer reaction as effectively. This reduction in the forward rate is likely due to restrictions in the hydrogen bonding network of water as well as the simultaneous need for the water molecules to solvate the ionic sulfonate groups that are part of the interfacial region. Solvation of the proton requires hydrogen bond network structural reorganization. Experiments on water in both AOT and Nafion show that the time scale of hydrogen bond structural rearrangement increases substantially as the size of the water regions become small,<sup>29–32,34,35</sup> which suggests an inability of the nanoscopic water to rapidly reconfigure to accommodate a newly generated proton. The back reaction, or  $k_{-1}$ , increases as the hydration level decreases primarily because the proton diffusion constant is highly sensitive to the hydrogen bonding environment. Again, as the water regions shrink in size and water molecules become less mobile, they are less able to structurally rearrange their hydrogen bonding network to permit proton transport. The decrease in the proton diffusion constant can be related to the increase in the back-reaction rate constant by eq 10. Measurements of the proton conductivity relative to the hydration level of Nafion show that the proton diffusion constant is greatly reduced at low water content, which supports the interpretation given here.<sup>21</sup>

Like the steady-state fluorescence spectra in Figure 3, the time-resolved fluorescence decays for the protonated state of HPTS in Nafion and AOT at the same hydration levels are qualitatively similar. The rate constants,  $k_1$  and  $k_{-1}$ , for the two systems at higher hydration levels also show a rough correspondence. However, the back-reaction rate constants tend to be larger in Nafion than in AOT at a given hydration level. This is the most apparent at low hydration levels. While AOT water nanopools and Nafion channels are being compared, it is important to recognize that the two systems have water in cavities with different topologies. AOT has monodispersed spherical water pools,<sup>17,18</sup> while neutron scattering experiments indicate that Nafion has an extended tortured channel structure.<sup>2,56,57</sup> In many other contexts, it is well documented that

(52) Ediger, M. D.; Fayer, M. D. *J. Chem. Phys.* **1983**, *78*, 2518–2524.

(53) Ediger, M. D.; Fayer, M. D. *J. Phys. Chem.* **1984**, *88*, 6108–6116.

(54) Baumann, J.; Fayer, M. D. *J. Chem. Phys.* **1986**, *85*, 4087–4107.

(55) Petersen, K. A.; Fayer, M. D. *J. Chem. Phys.* **1986**, *85*, 4702–4711.

(56) Rubatat, L.; Gebel, G.; Diat, O. *Macromolecules* **2004**, *37*, 7772–7783.

(57) Gebel, G. *Polymer* **2000**, *41*, 5829–5838.

the topology of a transport system has a substantial influence on transport kinetics.<sup>52,54,58,59</sup> With the differences in topology in mind, it is still useful to note that the proton-transfer dynamics measured in the Nafion sample with the greatest water content,  $\lambda = 8$ , is most similar to the  $w_o = 10$  AOT reverse micelle. The water pool in a  $w_o = 10$  AOT reverse micelle is 4 nm in diameter. While the topology of the water regions is very different in Nafion and AOT, 4 nm can be taken as a size scale for the water region in  $\lambda = 8$  Nafion. This size is consistent with estimates made using a variety of methods.<sup>4,13,60–62</sup>

**Oriental Relaxation.** Previous time-resolved anisotropy studies of a probe molecule in micelles<sup>63–65</sup> have shown that the observed anisotropy decay can be attributed to two different motions: one is related to the motion of the probe molecule inside the micelle and the other is related to the rotation of the micelle as a whole. Because the two motions are independent of one another, the orientational correlation function can be factored into a product of two correlation functions. The anisotropy can then be expressed as

$$r(t) = \frac{2}{5} C_p(t) C_m(t) \quad (12)$$

where  $C_p(t)$  and  $C_m(t)$  are the orientational correlation functions for the probe molecule and the micelle, respectively.

The orientational diffusion of large spherical systems, such as micelles, can often be described quite accurately with the Debye–Stokes–Einstein equation with stick boundary conditions. Therefore

$$C_m(t) = \exp(-t/\tau_m) \quad (13)$$

where  $\tau_m$  is the orientational relaxation time of the micelle, given by

$$\tau_m = \eta V_m / k_B T \quad (14)$$

Here,  $\eta$  is the solvent viscosity,  $V_m$  is the hydrodynamic volume of the micelle,  $k_B$  is Boltzmann's constant, and  $T$  is the absolute temperature.

Because HPTS undergoes excited-state proton transfer, the methoxy derivative of HPTS, MPTS (see Figure 2), was used for anisotropy measurements. Both the absorption and emission spectra of the protonated state HPTS and MPTS<sup>32</sup> are virtually identical, and the methoxy substitution should have no effect on the position of the chromophore in the sample.

To compare anisotropy measurements made in AOT reverse micelles to the measurements made in Nafion, the contribution to the anisotropy decay from the micelle orientational diffusion must be removed. Small-angle neutron studies show that the size of AOT reverse micelles is relatively independent of the solvent used for the organic phase.<sup>66</sup> The micelle volume was

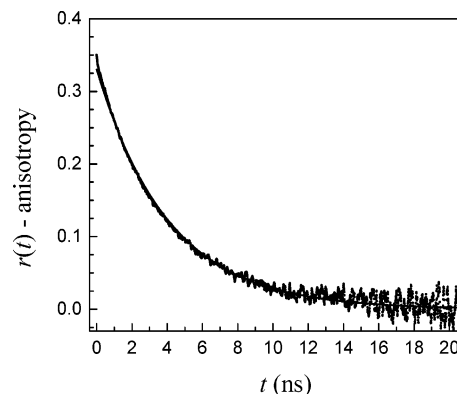


**Figure 7.** Anisotropy decay of MPTS in a  $w_o = 1$  AOT reverse micelle. The solid line shows the fit to a single-exponential decay. The anisotropy decay for  $w_o = 1$  is caused solely by the reorientation of the entire reverse micelle.

obtained from the previously measured size vs  $w_o$  in cyclohexane,<sup>67</sup> and corrected for the size of the MPTS molecule. The smallest AOT reverse micelle,  $w_o = 1$ , has a total radius of 1.7 nm. The hydroscopic radius of MPTS is approximately 0.5 nm, and the measured radius of the  $w_o = 1$  water pool without a probe molecule is  $\sim 0.6$  nm. As discussed above, like HPTS, MPTS is located in the water nanopool rather than in the reverse micelle wall. The inclusion of the relatively large probe molecule into the small nanopool should increase the radius of the AOT reverse micelle. The blue-shifted fluorescence spectrum of HPTS in the  $w_o = 1$  AOT reverse micelle (Figure 3A) indicates restricted solvation relative to all larger micelles. From this observation, it is reasonable to expect little or no reorientation of the MPTS chromophore in the  $w_o = 1$  AOT reverse micelle within its excited-state lifetime.

The anisotropy decay of MPTS measured in a  $w_o = 1$  reverse micelle is a single-exponential decay with a decay time of 4.0 ns as shown in Figure 7. The fact that single-exponential anisotropy decay is observed for the  $w_o = 1$  reverse micelle also gives evidence that the MPTS molecule does not undergo orientational relaxation in the water nanopool to any measurable extent because such relaxation would be restricted orientational diffusion, which produces nonexponential decays (see below).

An orientational relaxation time of 4.0 ns is obtained from the Debye–Stokes–Einstein equation (eq 14) with the viscosity of heptane (0.417 cP<sup>68</sup>),  $T = 298$  K, and adjusting the radius of the micelle to equal 2.1 nm. The measured size of the  $w_o = 1$  AOT reverse micelle is 1.7 nm, a difference of 0.4 nm. This increase in size is close to the hydrodynamic radius of MPTS. The orientational relaxation times for reverse micelles with  $w_o > 1$  were obtained by adding 0.4 nm to their previously reported radii.<sup>67</sup> This approximation to account for the size of the MPTS molecule may not be totally accurate for the larger reverse micelles, but since the reorientation time in the Debye–Stokes–Einstein equation grows linearly with volume, this correction is only important for the smallest micelles.

Figure 8A shows the anisotropy decay of MPTS in AOT, with the orientational relaxation of the entire reverse micelle removed, and Figure 8B shows the equivalent measurements made in Nafion. (In Nafion no correction equivalent to removing the micelle rotation is necessary.)

(58) Odagaki, T.; Lax, M. *Phys. Rev. B* **1981**, *24*, 5284–5294.

(59) Loring, R. F.; Fayer, M. D. *Chem. Phys.* **1982**, *70*, 139–147.

(60) Orfino, F. P.; Holdcroft, S. J. *New Mater. Electrochem. Syst.* **2000**, *3*, 285–290.

(61) Dreyfus, B.; Gebel, G.; Aldebert, P.; Pineri, M.; Escoubes, M.; Thomas, M. J. *Phys. (Paris)* **1990**, *51*, 1341–1354.

(62) Lehmani, A.; Durand-Vidal, S.; Turq, P. *Appl. Polym. Sci.* **1998**, *68*, 503–508.

(63) Wittouck, N.; Negri, R. M.; Ameloot, M.; De Schryver, F. C. *J. Am. Chem. Soc.* **1994**, *116*, 10601–10611.

(64) Wong, W.; Thomas, J. K.; Gratzel, M. J. *Am. Chem. Soc.* **1976**, *98*, 2391–2397.

(65) Eicke, H.; Zinsli, P. E. *J. Colloid Interface Sci.* **1977**, *65*, 131.

(66) Almgren, M.; Johannsson, R. *J. Phys. Chem.* **1992**, *96*, 9512–9517.

(67) Maitra, A. *J. Phys. Chem.* **1984**, *88*, 5122.

(68) Wiswanath, D. S.; Natarajan, G. *Data Book on the Viscosity of Liquids*; Hemisphere Publishing Corp.: Bristol, PA, 1989.



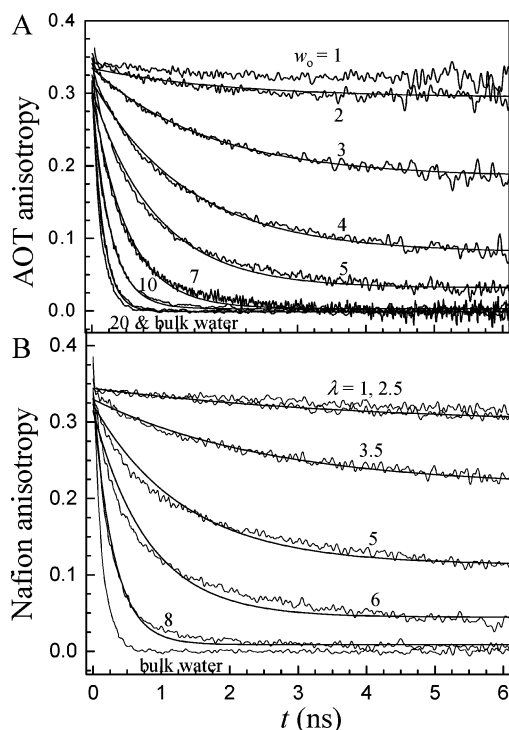


**Figure 8.** (A) Anisotropy decays of MPTS in the water nanopools of AOT reverse micelles (corrected for the anisotropy decay of the entire micelle). (B) Anisotropy decays of MPTS in Nafion.

The initial anisotropy for all of the samples extrapolate to slightly under 0.35, which is in agreement with previous steady-state anisotropy studies of HPTS in glycerol at low temperature.<sup>21</sup> Much like the comparison of the steady-state fluorescence spectra and the time-resolved proton-transfer kinetics of HPTS in AOT and Nafion, the anisotropy decays of MPTS in these two materials also demonstrate a qualitative correspondence at an equivalent hydration level. At low hydration, the orientational diffusion is restricted, which leads to a very slow decay time with a large residual anisotropy at long times. Under high hydration this long-time residual anisotropy disappears and the orientational dynamics become much more like those of bulk water.

To compare the data displayed in the two figures on a more quantitative level, the data sets were fit to a single-exponential decay with an offset.

$$r(t) = a \exp(-t/\tau_p) + b \quad (15)$$

Equation 15 has the form obtained from the wobbling-in-a-cone model, which has been successful for describing restricted orientational diffusion of molecules in reverse micelles and other confined environments.<sup>69–71</sup> In this model, the molecule is free to diffuse randomly within a cone of semiangle  $\theta$ . This semiangle is related to eq 15 by

$$\sqrt{b/(a+b)} = \frac{1}{2} \cos(\theta)(1 + \cos(\theta)) \quad 0 \leq \theta \leq 90^\circ \quad (16)$$

In systems where there are no angular restrictions on orientational diffusion, the decays reflect a second-order Legendre polynomial and the observed decay time,  $\tau_p$ , can be related to

**Table 2.** Wobbling-in-a-Cone Parameters for MPTS in AOT and Nafion

(A) MPTS in AOT					
$w_0$	$\tau_p$ (ns <sup>-1</sup> )	$a$	$b$	$\theta$	$D_p$ (ns <sup>-1</sup> )
bulk	0.13	0.32			1.3
20	0.16	0.32			1.0
10	0.27	0.31			0.62
7	0.51	0.31			0.33
5	0.93	0.27	0.032	63	0.24
4	1.4	0.23	0.080	52	0.12
3	1.7	0.15	0.18	35	0.057
2	2.0	0.04	0.29	17	0.012
(B) MPTS in Nafion					
$\lambda$	$\tau_p$ (ns <sup>-1</sup> )	$a$	$b$	$\theta$	$D_p$ (ns <sup>-1</sup> )
8	0.30	0.32	0.01	75	0.56
6	0.81	0.27	0.045	60	0.26
5	1.3	0.21	0.11	46	0.12
3.5	2.6	0.11	0.21	30	0.028
2.5	4.0	0.047	0.30	18	0.006

the orientational diffusion constant by

$$D_p = \frac{1}{6\tau_p} \quad (17)$$

However, when there are angular restrictions, the relationship between the orientational diffusion constant and the measured decay time takes on a more complicated form

$$D_p = \frac{x^2(1+x)^2\{\ln[(1+x)/2] + (1-x)/2\}}{\tau_p(1-Q^2)[2(x-1)]} + \frac{(1-x)(6+8x-x^2-12x^3-7x^4)}{24\tau_p(1-Q^2)} \quad (18)$$

where  $x = \cos(\theta)$  and

$$Q = \frac{1}{2} \cos(\theta)(1 + \cos(\theta)) \quad (19)$$

Table 2 gives the fitting parameters from this model. The anisotropy relaxation time of the largest reverse micelle ( $w_0 = 20$ ) is near that of bulk water. Experiments measuring water orientational relaxation in AOT  $w_0 = 20$  reverse micelles showed that for this size reverse micelle (and larger) the reorientation dynamics are virtually indistinguishable from those of bulk water.<sup>32,35</sup> The probe molecule's reorientation slows as the water pool shrinks in size. The decay is single exponential for all reverse micelles larger than  $w_0 = 5$ , which corresponds to a water pool of approximately 2.5 nm in diameter. Much like the ESPT measurements, the anisotropy relaxation dynamics for the largest Nafion hydration,  $\lambda = 8$ , lies in between what is measured for  $w_0 = 10$  and  $w_0 = 7$ . The diffusion constants and angles for MPTS in Nafion of hydrations of  $\lambda = 5$  and  $\lambda = 3.5$  are most comparable to  $w_0 = 4$  and  $w_0 = 3$ , respectively. It should also be noted that the fits to the wobbling-in-a-cone model for all of the AOT samples are quite reasonable but the fits for the intermediate hydration levels of Nafion are not nearly as good.

## Concluding Remarks

Through proton transport measurements using the photoacid HPTS and anisotropy measurements on MPTS, the water

(69) Lipari, G.; Szabo, A. *Biophys. J.* **1980**, *30*, 489–506.

(70) Kinoshita, K.; Kawato, S.; Ikegami, A. *Biophys. J.* **1977**, *20*, 289–305.

(71) Quitevis, E. L.; Marcus, A. H.; Fayer, M. D. *J. Phys. Chem.* **1993**, *97*.

environment of sodium-substituted Nafion appears to be quite similar to the water pools found in AOT reverse micelles at a similar hydration level. The ESPT measurements are in agreement with many previous macroscopic proton conductivity studies<sup>5,21,72–74</sup> that show the proton diffusion constant is reduced dramatically as the hydration level is decreased in Nafion. This is most likely due to a change in the hydrogen bonding network of water as the water pools are reduced in size. The restrictions on hydrogen bonding prevent the charge pair formed in the proton-transfer process from being rapidly solvated, which is consistent with the direct studies of hydrogen bond dynamics in the confined water systems.<sup>29–35</sup> The inability of the nanoscopic water to readily solvate the proton shifts the equilibrium to less deprotonation and reduces the rate of the reaction.

The constrained hydrogen bonding environment also causes the orientational diffusion to become slower for MPTS in Nafion as the water channels become smaller. In addition to the orientational diffusion constant decreasing dramatically when the hydration level is reduced, the motion becomes restricted due to the constraints placed on reorientation by topology of the aqueous cavity and the lengthening of the time scale for the hydrogen bond network structural relaxation. The result is a significant long-time offset in the anisotropy decay, which is

- (72) Zawodzinski, T. A., Jr.; Springer, T. E.; Davey, J.; Jester, R.; Lopez, C.; Valerio, J.; Gottesfeld, J. *J. Electrochem. Soc.* **1993**, *140*, 1981–1985.  
(73) Cappadonia, M.; Erning, J. W.; Stimming, U. *J. Electrochem. Soc.* **1994**, *376*, 189–193.  
(74) Cappadonia, M.; Erning, J. W.; Saber Niaki, S. M.; Stimming, U. *Solid State Ionics* **1995**, *77*, 65–69.

initially seen as the size is reduced at approximately the same hydration level in Nafion ( $\lambda \leq 6$ ) and AOT ( $w_o \leq 5$ ).

The results presented here show that the nature of the water environment experienced by the probe molecules HPTS and MPTS are very similar. Recent experiments on water in AOT and a nonionic head group reverse micelle with the same size nanopool show that the nature of the head group matters to some extent, but that the dynamics of the hydrogen bonding network are largely determined by confinement to a nanometer size. Here the sizes of the water cavities are approximately the same and the head groups are the same. The results are proton transport and orientational relaxation that are very similar even if the topologies of the water cavities are not identical. The effective volume of water that surrounds the probe molecules in Nafion at a given  $\lambda$  value is similar to the size of an AOT reverse micelle at an equivalent  $w_o$ . Therefore, the relationship between  $w_o$  and reverse micelle size for AOT (eq 2) could provide a rough approximation to estimate the size of the aqueous domains which are sampled by a highly hydrophilic molecule in Nafion. In addition to examining the nature of water in Nafion, the results presented here give the first molecular level picture of proton transport in Nafion water channels.

**Acknowledgment.** This work was supported by the Department of Energy (DE-FG03-84ER13251). D.B.S thanks the NSF for a graduate fellowship. D.E.M. thanks the NDSEG for a graduate fellowship. The authors would also like to thank William Childs for his initial help with TCSPC measurements.

JA071939O